Available online at www.sciencedirect.com

ScienceDirect

IFAC Papers Online CONFERENCE PAPER ARCHIVE

IFAC-PapersOnLine 49-11 (2016) 633–640

Model-based development of combustion-engine control and optimal calibration for driving cycles: general procedure and application

Rolf Isermann*. Heiko Sequenz*

**Institute of Automatic Control and Mechatronics, Technische Universität Darmstadt, 64283 Darmstadt, Germany (risermann@iat.tu-darmstadt.de)*

Abstract: A systematic procedure for the model-based design of multi-variable control functions of internal combustion engines is described taking the stationary as well as the dynamic behavior into account. First, the workflow for the data-driven identification with test benches is described to result in stationary and dynamic nonlinear engine models. A multi-goal optimization then yields an optimal control with different criteria for fuel consumption and emissions. Then, as an example, the model-based control optimization of fuel consumption and emissions is considered with local and global quasi-stationary optimization for driving cycles, based on test measurements of a four-cylinder diesel engine, and including model uncertainties and series variations.

Keywords: Internal Combustion Engine Control, Optimal Calibration, Fuel Consumption, Emission Models, Driving Cycles.

1. INTRODUCTION

The increasing economic and ecologic requirements to reduce fuel consumption and emissions, and to provide detailed diagnosis functions are strong challenges for the further development of internal combustion engines. Many basic improvements are reached by basic design measures like multiple injections, mixture formation, charging, combustion methods, exhaust gas after-treatment, and in general downsizing. A significant part of the progress is reached by an increase of variabilities like, e.g. adjustable pre-, main- and post-injections, variable rail pressure, adjustable exhaust-gas recirculation and variable turbochargers. These higher variabilities result in an increase of actuators and additional sensors, like for example the air excess factor λ, NOx, charging pressure, combustion pressure, and exhaust-gas temperatures. As a consequence the structure and the control functions of the electronic control unit (ECU) become rather complex and need a model-based design with physical-based and experimentally gained mathematical models. This contribution briefly summarizes ways and methods from test bench measurements to model-based design of multi-variable control functions. Then, an example for model-based control of a turbocharged diesel engine is shown with local and global driving-cycle-oriented optimization of the control with regard to weighted minimal fuel consumption and emissions.

2. EXPERIMENTAL MODELLING OF THE STATIONARY AND DYNAMIC BEHAVIOR

The basic structure of mathematical models for the stationary and dynamic behavior of combustion engines can be gained from physical laws via the statement of balance equations, constitutive and phenomenological relations, Guzzella and Onder (2010), Kiencke and Nielsen (2005), Eriksson and Nielsen (2014), Isermann (2014). For example, the behavior of the air path, the cylinder pressure for the charging cycles, or the dynamic torque generation can be described with good accuracy. However, modeling the details of the fuel injection and succeeding combustion phases, forth and back flows through the valves, temperature distribution in the engine block and the development of raw emissions is usually not possible with simple theoretical models only. Additionally, many parameters are not or not precisely known. Therefore, suitable, not too complex but precise models have to be obtained by experimental modeling of combustion engines through the evaluation of measurements, preferable on engine test benches. Then semi-physical models result if the model structure follows from theoretical modeling (grey-box models) or pure experimental models (black-box models) if the input-output behavior is approximated by applying identification and parameter-estimation methods. A general workflow for obtaining data-based models on test benches is depicted in Fig. 1. First the operating boundaries (variation space) have to be determined experimentally to stay within given limits and to avoid damage. Then, stationary or dynamic test signals have to be specified, measurements have to be performed, data analyzed and filtered, models calculated, analyzed and validated. For these tasks special software tools were created, see e.g. Alberer et al. (2012), Isermann and Münchhof (2011), Isermann (2010), Kruse et al (2010), Röpke (2005). Fig. 2 gives a survey on the identification methods for modeling of the stationary and dynamic (transient) behavior of combustion engines.

2.1 Identification of the stationary behavior

The most direct way to determine the stationary behavior of a nonlinear process with one input U and one output Y is to take samples in steady state for $Y(k)$ and different $U(k)$ for the discrete time $k = 0,1,\ldots, N-1$ and to represent them in a

Peer review under responsibility of International Federation of Automatic Control.
10.1016/j.ifacol.2016.08.092

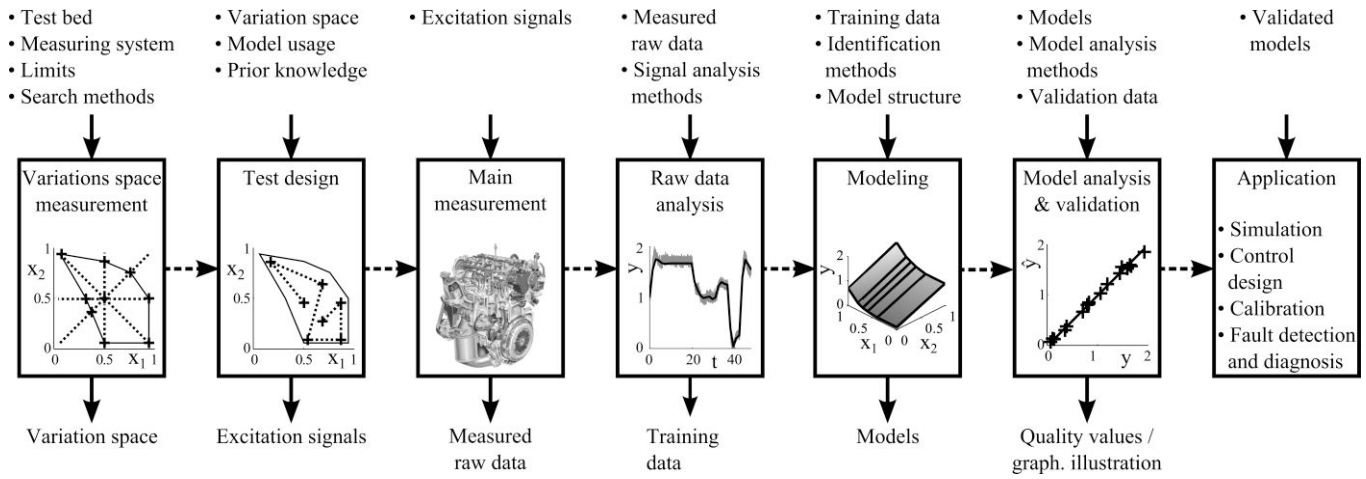

Fig. 1. Workflow for experimental engine modeling with test benches

graph. However, because of noisy measurements a regression procedure has to be applied. In the case of several inputs

$$\mathbf{U}^{\mathrm{T}} = \left[U_1, U_2, \ldots, U_{\mathrm{p}}\right] \tag{1}$$

$$Y = f\left(\mathbf{U}\right) \tag{2}$$

the output Y can be represented in a multidimensional look-up table or map. The measurements are taken for all combinations of the inputs. Grid-based look-up tables are the most common type of nonlinear static models used in practice for one or two inputs and are a suitable means for the storage of nonlinear static mappings in the ECU (electronic control unit). The most widely applied method of obtaining the data point values is to position measurement data points directly on the grid.

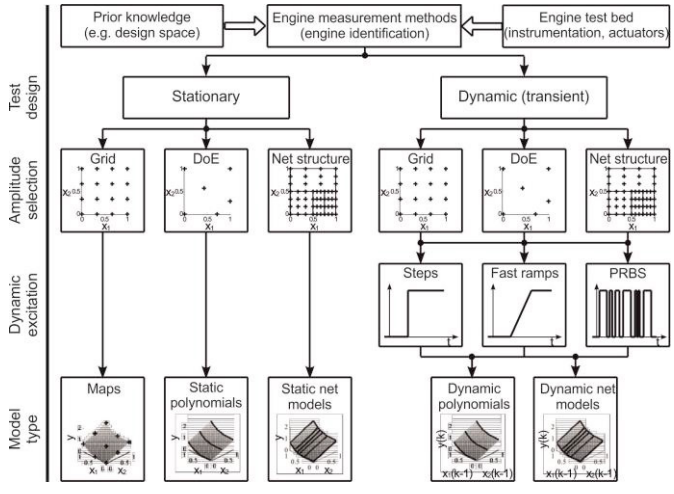

Fig. 2. Survey of identification methods for combustion engines, Isermann (2014)

Grid-based look-up tables belong to the class of non-parametric models. The described model structure has the advantage that a subsequent adaptation of single data point heights, e.g. due to changing environmental conditions can be directly realized. The main disadvantage of look-up tables is the exponential growth of the number of data points with an increasing number of inputs. Therefore, grid-based look-up tables are in practical applications mostly restricted to one- and two-dimensional input spaces. However, different ways do exist to extend them to multi-inputs and to use them for control, see e.g. Sequenz et al. (2012). An alternative are parametric model representations, like polynomial models or neural networks which require less model parameters to approximate a given input output relationship. Hence, a parametric equation is assumed, e.g. in form of a polynomial and output measurements $Y(k)$ are taken for different inputs $U(k)$ spanning the range of interest, where $k = 0, 1, \ldots, N\text{-}1$ is (here) the running number. For one input and one output at sample k this yields

$$Y\left(k\right) = K_0 + U\left(k\right) K_1 + U^2\left(k\right) K_2 + \cdots + U^{\mathrm{q}}\left(\mathrm{k}\right) K_{\mathrm{q}} \tag{3}$$

Defining the vectors

$$\begin{aligned} \mathbf{U}\left(k\right) &= \left[1 U\left(k\right) U^2\left(\mathrm{k}\right) \ldots U^{\mathrm{q}}\left(k\right)\right] \\ \mathbf{K}^{\mathrm{T}} &= \left[K_0 K_1\ K_2 \ldots K_{\mathrm{q}}\right] \end{aligned} \tag{4}$$

leads with k = 0, …, N-1 to a regression model

$$\mathbf{Y} = \mathbf{U}\mathbf{K} + \mathbf{n} \tag{5}$$

where $\mathbf{U}$ is a N x q matrix and $\mathbf{Y}$ a vector of dimension N and $\mathbf{n}$ is a noise vector. Introducing the equation error a minimization of the sum of squared errors then yields the least squares estimate

$$\hat{\mathbf{K}} = \left[\mathbf{U}^{\mathrm{T}}\mathbf{U}\right]^{-1} \mathbf{U}^{\mathrm{T}}\mathbf{Y}. \tag{6}$$

For several inputs the vectors can be expanded. The selection of the inputs may be based on so-called design of experiment (DoE) methods, Röpke (2005). Other approaches are neural networks as multilayer perceptrons (MLP) and radial basis functions (RBF), see e.g. Isermann and Münchhof (2011), Isermann (2010). However, finding an appropriate structure and convergence behavior may cause problems. A further disadvantage is the lack of physical interpretability. An alternative are local linear network models, like LOLIMOT. They consist of the superposition of weighted linear models and are on the one side flexible for multi-inputs and on the

other side transparent, see Isermann and Münchhof (2011), Isermann (2010), Nelles (2001).

2.2 Identification of the dynamic behavior

The identification of strongly nonlinear processes with single input and single output are primarily based on parameter-estimation methods by applying the method of least squares and their modifications. To determine the dynamic behavior the process has to be excited by appropriate test signals like step functions, fast ramp functions, sinusoidal or pseudo-random binary signals (PRBS), Fig. 2. Then, present and past inputs $u(k)$, $u(k\text{-}1)$,…, u $(k\text{-}N)$ and outputs $y(k)$, $y(k\text{-}1)$,…, y $(k\text{-}N)$, where $k=t/T_0$ is the discrete time, with T_0 the sampling time, have to be recorded. The nonlinear models usually have a special structure like Hammerstein- or Wiener-models or like dynamic multilayer perceptrons. Local linear models, like LOLIMOT or local nonlinear models, like LOPOMOT, Sequenz (2013), can directly be extended to dynamic net models, are well interpretable, and therefore better suited.

3 ENGINE CONTROL DEVELOPMENT AND CALIBRATION

The design and implementation of electronic control and diagnosis systems is highly interrelated with the design of the mechanics, thermodynamics and fluid mechanics of internal combustion engines. It belongs to the design of mechatronic systems and requires a systematic development across the classical boundaries which leads to a simultaneous or concurrent engineering in different domains, usually represented in V-development model.

The design and implementation of engine control systems can be divided in function development and function calibration. The workflow for a model-based control-function development is depicted in Fig. 3. Because of the high demands on low fuel consumption, emissions and driveability, the number of main engine control inputs increased to 5-10 and the number of considered outputs to 6-8. Therefore, the design and calibration of the engine control has evolved into a highly complex task.

3.1 Optimization for the stationary behavior

A first approach for the optimization of the stationary control of combustion engines is to select stationary operating points $(M_{\mathrm{eng,i}}, n_{\mathrm{eng,j}})$. Then, the torque $M_{\mathrm{eng}} = M$ in dependence on the speed $n_{\mathrm{eng}} = n$

$$\max_{\mathrm{u}} M(n, \mathbf{u}) \tag{7}$$

can be optimized with regard to the manipulated variables $\mathbf{u}$ (e.g. the injection angle and rail pressure) and then the manipulated variables $\mathbf{u}_{\mathrm{opt}}$ in form of static maps as a function of (M, n) or (m_{f}, n) can be stored. Alternatively the specific fuel consumption can be minimized

$$\min_{\mathrm{u}} b_{\mathrm{sfc}}(n, \mathbf{u}). \tag{8}$$

In both cases the emission concentrations, related to the distance d_{cyl} [km] or time interval t_{cyc} [h], per driving cycle have to be smaller than certain limits according to legislative requirements, like

$$\bar{m}_{\mathrm{CO}} \le \bar{m}_{\mathrm{CO,lim}};\ \bar{m}_{\mathrm{CH}} \le \bar{m}_{\mathrm{CH,lim}};\ \bar{m}_{\mathrm{NOx}} \le \bar{m}_{\mathrm{NOx,lim}};\ \bar{m}_{\mathrm{PM}} \le \bar{m}_{\mathrm{PM,lim}} \tag{9}$$

where $\bar{m}$ stands for a distance or work related emission measure, e.g. $\bar{m}_{\mathrm{NOx,d}}$ in [g/km] or $\bar{m}_{\mathrm{NOx,P}}$ [g/kWh], see Isermann (2014), Sequenz (2013). If there are only some few manipulated variables $\mathbf{u}$, the optimal adjustments of the manipulated variables $\mathbf{u}_{\mathrm{opt}}$ are then stored (manually) in the ECU as look-up tables in dependence on the operation points $(M_{\mathrm{i}}, n_{\mathrm{j}})$ or $(m_{\mathrm{f,i}}, n_{\mathrm{j}})$.

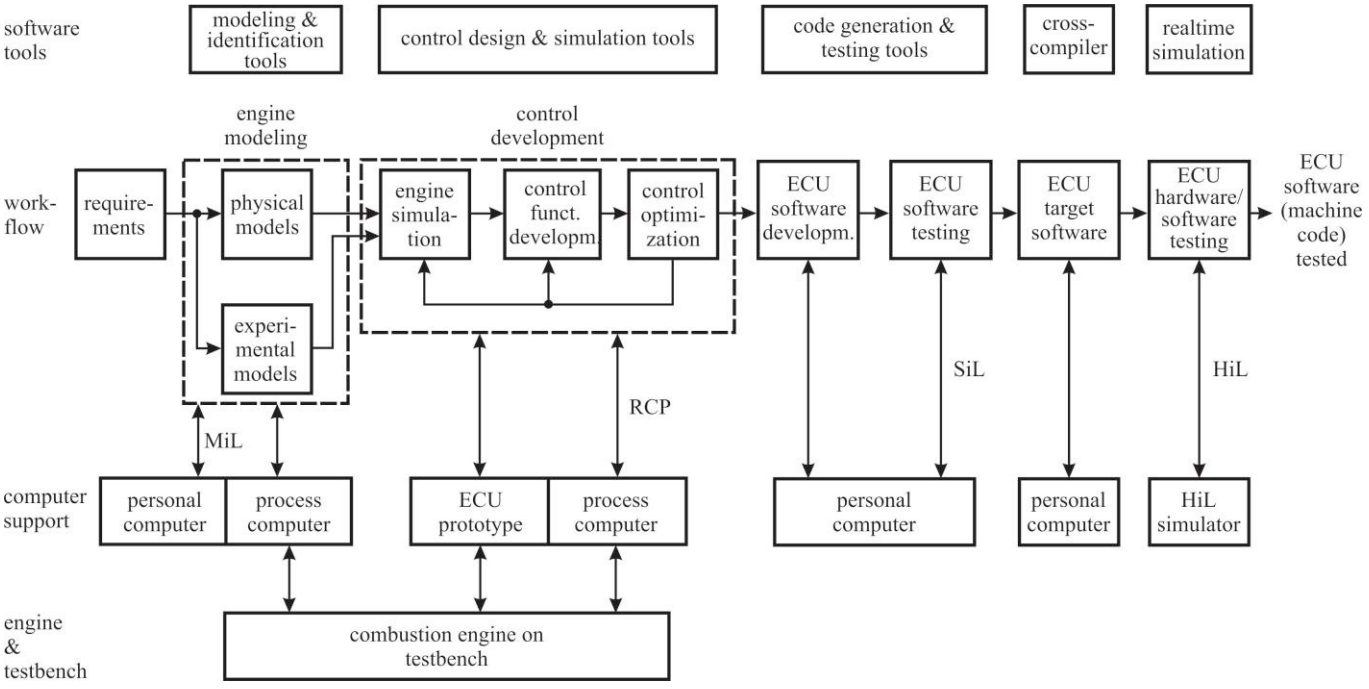

Fig. 3. Workflow for model-based control-function development

However, for the increased number of manipulated variables it is more efficient if the optimization of the calibration is not performed at the test bench, but with mathematical multi-input multi-output engine models on a computer. After the models are determined at the test bench by measurement and identification methods, see Section 2, the stationary maps for the manipulated variables $\mathbf{u}_{opt}$ can then be obtained with numerical optimization methods for selected operating points, Hafner (2002). In this case the engine behavior has to be measured and modeled only once and the calibration of the ECU is performed offline on personal computers. The achieved results have then to be validated with the engine at the test bench. If, however, the optimization has to consider a driving cycle, the engines together with a simulated transmission and vehicle have to be considered using programmed settings for torque and speed (corresponding to a virtual perfect driver) and a multi-criterion optimization has to be satisfied to minimize the fuel consumption for given constraints of emissions. Then a computer-based optimization with a mathematical dynamic engine model is required. The general task for the optimal calibration of engine control systems can be summarized by the formulation of a multivariable optimization criterion with different weights of the interesting output variables. For *one stationary operating* point with torque M_i and speed n_j a criterion with different weights of the output variables is

$$J\left(\mathbf{u}, M_i n_j\right) = [w_1 b_{\mathrm{sfc}}\left(\mathbf{u}\right) + w_2 m_{\mathrm{CO,P}}\left(\mathbf{u}\right) + w_3 m_{\mathrm{HC,P}}\left(\mathbf{u}\right) + \\ + w_4 m_{\mathrm{NOx}}\left(\mathbf{u}\right) + w_5 m_{\mathrm{PM,P}}\left(\mathbf{u}\right)] P_{ij} \Delta t_{ij} \quad (10)$$

with the power $P_{ij} = M_i \omega_j = M_i \pi n_j / 30$, brake specific fuel consumption b_{sfc} [g/kWh], and work-related emissions $m_{\mathrm{x,P}}$ in [g/kWh], Δt_{ij} time interval per run, and $\sum_{v=1}^{5} w = 1$. If stationary mathematical models of the engine are available, the optimization

$$\min_{\mathrm{u}} J\left(\mathbf{u}, M_{\mathrm{i}} n_j\right) \quad (11)$$

can be performed with numerical optimization methods to find the optimal manipulated variables $\mathbf{u}_{opt}$ (M_i, n_j) for each operating point (M_i, n_j). If real vehicle driving is considered, *several operating points* can be selected according to their frequencies of appearance. A further example for a driving cycle-oriented optimization with stationary engine models is given by Kötter (2008). The optimization criterion then becomes for, e.g. 10 operating points

$$m_{\mathrm{f}}\left(\mathbf{u}\right) = w_1 m_{\mathrm{f1}}\left(\mathbf{u}_1\right) + w_2 m_{\mathrm{f2}}\left(\mathbf{u}_2\right) + \cdots + w_{10} m_{\mathrm{f10}}\left(\mathbf{u}_{10}\right) \quad (12)$$

with several boundary conditions, like

$$m_{\mathrm{NOx}}\left(\mathbf{u}\right) = w_1 m_{\mathrm{NOx1}}\left(\mathbf{u}_1\right) + w_2 m_{\mathrm{NOx2}}\left(\mathbf{u}_2\right) + \cdots + \\ + \cdots + w_{10} m_{\mathrm{NOx10}}\left(\mathbf{u}_{10}\right) \le m_{\mathrm{NOx,lim}} \quad (13)$$

where $m_{\mathrm{NOx,lim}}$, $m_{\mathrm{PM,lim}}$ etc. are the legislative emission limits per cycle. In general, the raw emissions are considered if the goal is to optimize the control of the engine itself.

3.2 Optimization for the dynamic behavior

The increasing requirements for the reduction of fuel consumption and emissions and for the improvement of driveability need the inclusion of the dynamic engine behavior for the control design. For driving cycles like the NEDC the percentage of emissions during dynamic acceleration states is around 40…50 %. As the variables of the optimization criteria like fuel consumption, emissions and acceleration are influenced by the dynamic engine behavior, they have to be included in the optimization process, at least for high dynamic cycles as the WLTC. One possibility then is to minimize the fuel consumption over a driving cycle,

$$J_{\mathrm{dyn}}\left(\mathbf{u}(t)\right) = m_{\mathrm{f}}\left(\mathbf{u}(\mathrm{t})\right) = \int_0^{t_{\mathrm{dyn}}} \dot{m}_{\mathrm{f}}\left(\mathbf{u}(t)\right) dt \quad (14)$$

together with the boundary conditions like

$$m_{\mathrm{NOx}}\left(\mathbf{u}(t)\right) = \int_0^{t_{\mathrm{dyn}}} \dot{m}_{\mathrm{NOx}}\left(\mathbf{u}(t)\right) dt \le m_{\mathrm{NOx,lim}} \quad (15)$$

The optimization task is then concentrated on the optimization of a single variable m_{f} taking into account several constraints for the resulting emissions. However, the effect of the dynamic behavior depends strongly on the dynamic parts of the driving cycle. For the NEDC quasi-stationary optimization is sufficient, Mrosek (2016), because of its relative small accelerations.

4. MODEL-BASED QUASI-STATIONARY OPTIMIZATION OF FUEL CONSUMPTION AND EMISSIONS OF A DIESEL ENGINE FOR DRIVING CYCLES – AN EXAMPLE

4.1 Emission model structure

The engine emissions are modeled by a mean value model. Therefore the combustion process can be regarded as a cyclic batch process, depending only on the engine operation point, the air path states in the intake and a combustion feature describing the combustion process itself. The dynamic engine behavior, which is mainly introduced by the air path, is regarded separately, see Fig. 4. Thus, the air path and the combustion process can be modeled independently. For the air path dynamical model structures with semi-physical approaches, as described in Guzella, Onder (2010), can be applied. This contribution *focuses on the outcome of the combustion process* (raw emissions NOx, soot emissions and engine torque) which are modelled by an experimental approach. Since the combustion is regarded as a batch process, all dynamics in emission formation are covered by the dynamical air path. Thus, a stationary model structure for combustion can be applied. The inputs of the emission models and the torque model are the engine operation point (engine speed n_{eng} and injection quantity u_{inj}), the states of the air path at intake (air mass per cycle m_{air}, intake pressure $p_{2\mathrm{i}}$ and intake temperature $T_{2\mathrm{i}}$) and a combustion feature (crank angle of 50% mass fraction burnt φ_{Q50}, as one possibility to cover the effects of fuel injection). As the formation of soot mainly depends on the local availability of oxygen, the gas composition after combustion $x_{\mathrm{eng,out}}$ is included as alternative input to m_{air} for the soot model, Sequenz et al (2011).

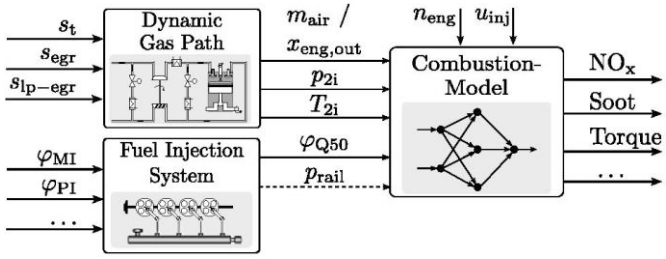

Fig. 4 Block diagram of the combined air path and combustion model. The dynamics in emission formation are covered by the dynamical air path, such that a stationary model structure can be applied for the combustion model.

The emission model structure consists of several *local models* which are superimposed to a *global model output*. The local models are identified for fixed engine operation points, distributed over the engine operation range, such that the relevant region of common test cycles is covered, see Fig. 5. For each operation point, the local driveability space is covered with measurements. This driveability space can then be described by a convex hull surrounding the measurements. Using this convex hull, an extrapolation measure can be constructed, indicating if the model operates in extrapolation or not, see Sequenz et al. (2010). This extrapolation measure is mandatory for the optimization algorithm to guarantee that the optimization results are reachable in practice.

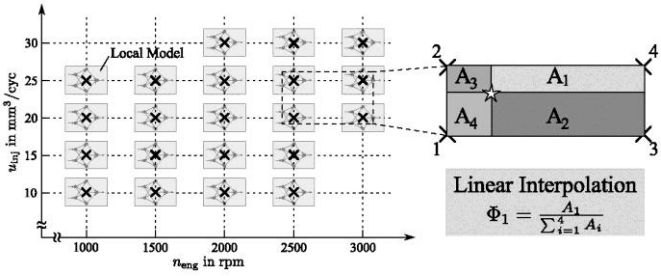

Fig. 5 Distribution of the local models in the engine operation range. Operation points in between the local models are modelled by a linear interpolation of the surrounding models

The local models are described by polynomials. The outputs of these local models are weighted by means of a linear interpolation Φ and summed up to a global model output, see Fig. 6. The weighting is determined by the engine operation point given as z-regressors. The local polynomials depend on the x-regressors, which are the remaining model inputs. The polynomial regressors are selected by an algorithm described in Sequenz (2009), which enables an adaption to the nonlinearity of the regarded output and increases thus the model quality. The output of the emission model is given by

$$y = \sum_{j=1}^{M} \Phi_j(n_{eng}, u_{inj})\ (w_{0,j} + w_{1,j}x_1 + w_{2,j}x_1x_2 + w_{3,j}x_i^2 + ...), \quad x_i \in \{m_{air}, p_{2i}, T_{2i}, \varphi_{Q50}\}. \tag{16}$$

Further descriptions of the emission models with training and validation results for stationary and dynamical data can be found in Sequenz et al. (2010), Mrosek et al. (2010).

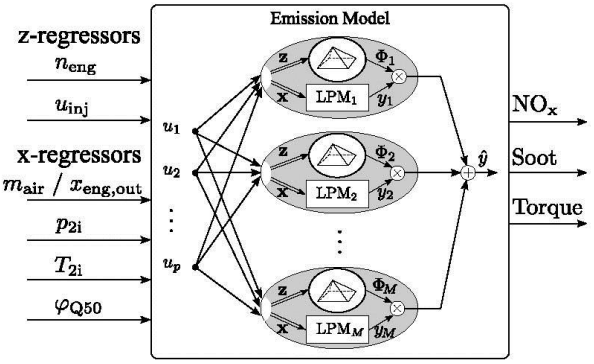

Fig. 6 Combustion model structure consisting of local polynomial models (LPM) with x-regressors as local model inputs and weighting functions determined by the z-regressors

Emissions such as NOx are measured as concentrations c_x in ppm, whereas the emission masses are relevant for the legislative regulations. Therefore, the following transformation to an emission mass flow rate in mg/s is applied

$$\dot{m}_x\,[\mathrm{mg/s}] = c_x\,[\mathrm{ppm}]\frac{m_{mol,x}\,[\mathrm{g/mol}]}{m_{mol,exh}\,[\mathrm{g/mol}]}\dot{m}_{exh,out}\,[\mathrm{kg/s}] \tag{17}$$

Herewith $m_{mol,x}$ is the molar mass of the measured emission and $m_{mol,exh}$ is the molar mass of the exhaust gas which can be simplified to the molar mass of air (28.96 g/mol). $\dot{m}_{exh,out}$ is the tailpipe gas mass flow rate and does therefore not include the recirculated exhaust gas. For NOx the molar mass is given as NO_2 equivalent (46.01 g/mol), see European Commission (2007). In contrast the soot concentration c_{soot} is measured in mg/m³ and needs therefore be transformed by

$$\dot{m}_{soot}\,[\mathrm{mg/s}] = \frac{c_{soot}\,[\mathrm{mg/m^3}]}{\rho_{exh,meas}\,[\mathrm{kg/m^3}]}\dot{m}_{exh,out}\,[\mathrm{kg/s}] \tag{18}$$

where $\rho_{exh,meas}$ is the density of the gas in the measuring cell.

4.2. Local Optimization

For optimization the relevant region of the NEDC is regarded, Fig. 7. For a local optimization, each operation point is optimized separately. As loss function a multi-objective criterium is applied

$$\min_x J_{local} = k_{NOx}\dot{m}_{NOx}(x) + k_{soot}\dot{m}_{soot}(x) \quad \text{for each } \{n_{eng}, u_{inj}\} = \text{const.} \tag{19}$$

The variable x is 4-dimensional and contains the local model inputs $\mathbf{x} = [m_{air}, p_{2i}, \varphi_{Q50}, T_{2i}]$. The weights k_{NOx} and k_{soot} are chosen such that

$$k_{NOx} = 1 - k_{soot} \text{ and } k_{NOx} \in [0,1] \tag{20}$$

It is also possible to include further outputs in the loss function. However, the selection of weights is then complicated. In the following, (19) is optimized with varying weights. Since the emissions NO_x and soot are weighted with

the ratio 5 to 180 mg/km for the EU5 legislative limits, the distribution of the weights is chosen with respect to

$$k_{\mathrm{NOx}} = \frac{\frac{1}{35}(36^{2\tilde{k}_{\mathrm{NOx}}} - 1)}{37} \tag{21}$$

and $\tilde{k}_{\mathrm{NOx}}$ equidistantly distributed on [0,1], Sequenz (2013). Thus, for $\tilde{k}_{\mathrm{NOx}} = 0$ only soot is optimized, for $\tilde{k}_{\mathrm{NOx}} = 1$ only NO_x is optimized and for $\tilde{k}_{\mathrm{NOx}} = 0.5$ the weighting of NO_x to soot is 1 to 36 which corresponds to the EU5 limit values 5 to 180 mg/kg. As boundary condition it is in each optimization step ensured that **x** is in the driveability space defined by the convex hull around the measurements in the regarded operation point. Thus, it can be guaranteed that the optimization results are reachable in practice. Fig. 8 shows the optimization results of (19) for initial values taken on the one hand from a-priori knowledge and on the other hand from the centre of gravity of the driveability space.

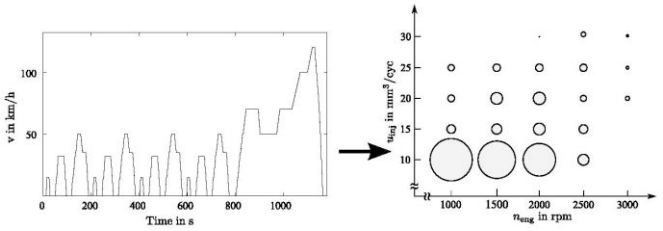

Fig. 7 New European Driving Cycle (NEDC) and the derived weights for each operation point for the global optimization (indicated by the size of the circles).

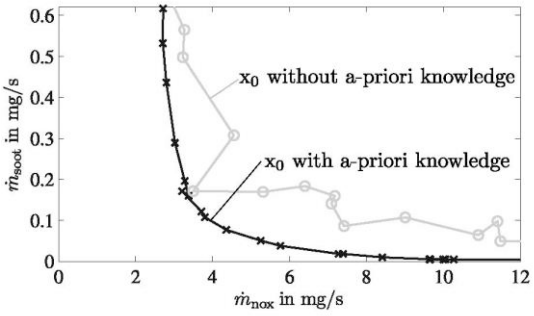

Fig. 8 Results for the local optimization of NO_x and soot emissions with regard to the selection of initial values for n_{eng}=2000 rpm and u_{inj}=25 mm^3/cyc. Grey: initial values from the centre of the driveability space; black: initial values taken from a previous optimization with a global optimization algorithm.

In both cases a local optimization algorithm is applied. It can be seen that the algorithm runs for several weights in a local minimum, if initial values are taken from the centre of the driveability space. The results with initial values taken from a-priori knowledge are however superior. This strong dependency on the initial values is mainly due to the nonlinear boundary conditions defined by the convex hull of the driveability space, which traps the local optimization algorithm in a local minimum on the boundary of the convex hull. The dependency on the initial values can be overcome if a global optimization algorithm is applied.

4.3 Consideration of model uncertainties and series variations

A problem for engine calibration is the transferability of the achieved results from the prototype engine to a series of engines. This is due to series variations which alter the optimal setpoints for each assembly. Further problems for model based optimization arise from model uncertainties which may permit better results than realisable in practice. Both uncertainties can be considered to maintain a sufficient distance to the limiting values. The model uncertainties are determined by the simulation qualities of the models in the region of the predicted optimum. Therefore, the measurement data from model parameterization $N_{x,y}$ is used. From these sets, the 5 neighbouring points to the optimum x are determined by the distance

$$d(x, x_i) = \left\| \frac{x - x_i}{\Delta x} \right\|_2 \quad \text{with } x_i \in N_{x,y} \tag{22}$$

and x is the optimal setpoint of the variables.

Δx normalises the four dimensions by the maximum and minimum measured values. Then, the model outputs $\hat{y}_i$ at these neighbouring points are compared to the measured output values y_i. The standard deviations of $|y_i - \hat{y}_i|$ give then the model uncertainties σ.(x). For consideration of series variations, the derivatives of the emission models $d\dot{m}_{\mathrm{NOx}}(x)/dx$ and $d\dot{m}_{\mathrm{soot}}(x)/dx$ are regarded. These can be calculated, since the local models are described by polynomials. The variances in each dimension are then taken from sensor accuracies based on data sheets

$$\sigma_{\mathrm{sensor}} = [0.004, 0.02, 1, 2] \text{ in } [\text{g/cyc, bar, °CS, °C}]. \tag{23}$$

In a similar way also variations of the engine itself can be taken into account. From this the optimization criterion of (19) can be reformulated considering the uncertainties

$$\min_x J_{\mathrm{local}} = k_{\mathrm{NOx}} \left(\dot{m}_{\mathrm{NOx}}(x) + \sigma_{\mathrm{NOx}}(x) + \left| \frac{d\dot{m}_{\mathrm{NOx}}(x)}{dx} \right| \sigma_{\mathrm{sensor}} \right) + k_{\mathrm{soot}} \left(\dot{m}_{\mathrm{soot}}(x) + \sigma_{\mathrm{soot}}(x) + \left| \frac{d\dot{m}_{\mathrm{soot}}(x)}{dx} \right| \sigma_{\mathrm{sensor}} \right) \tag{24}$$

The absolute values of the derivatives ensure that the worst case is regarded. However, the consideration of uncertainties does affect the local optimization results only slightly. It is more important for a global optimization.

4.4 Global optimization

For a global optimization all M operating points are regarded simultaneously. To gain the weights k_j for the contribution of each operating point to the loss function, a certain test cycle needs to be assumed. Here the NEDC is regarded and the resulting weights are indicated by the size of the circles in Fig. 7. The objective is to optimise the brake specific fuel

consumption bsfc over the test cycle, while fulfilling the legislative boundary conditions

$$\min_x J_{\text{global}} = \frac{\sum_{\text{j=1}}^{M} k_j u_{\text{inj,j}}}{\sum_{\text{j=1}}^{M} k_j \frac{2\pi n_{\text{eng,j}}}{60} M_j(x)} \text{ with } \begin{matrix} \sum_{\text{j=1}}^{M} k_j \dot{m}_{\text{NOx},j}(x) \le \text{NO}_{\text{x,limit}} \\ \sum_{\text{j=1}}^{M} k_j \dot{m}_{\text{soot},j}(x) \le \text{soot}_{\text{limit}} \end{matrix} \tag{25}$$

where M_j is the torque of the j-th local model. Since the injected fuel mass $u_{\text{inj,j}}$ is constant for a given engine operation point j, the loss function can be reformulated to

$$\max_x J_{\text{global}} = \sum_{\text{j=1}}^{M} \frac{2\pi n_{\text{eng,j}}}{60} M_j(x) \text{with} \begin{matrix} \sum_{\text{j=1}}^{M} k_j \dot{m}_{\text{NOx},j}(x) \le \text{NO}_{\text{x,limit}} \\ \sum_{\text{j=1}}^{M} k_j \dot{m}_{\text{soot},j}(x) \le \text{soot}_{\text{limit}} \end{matrix} \tag{26}$$

Hence, the maximisation of a weighted sum of the local torque is the objective of the global optimization. As all inputs **x** of the loss function are optimized simultaneously, a high-dimensional problem arises. Since M=21 local models are regarded and 4 local inputs are optimized, the problem is of 84 dimensions. It is therefore essential to have good initial values, wherefore a local optimization is recommended previous to a global optimization. Local model uncertainties and series variations sum up to a global uncertainty and do deteriorate the produced raw emissions over a test cycle. The summed up emissions for a test cycle are illustrated in Fig. 9.

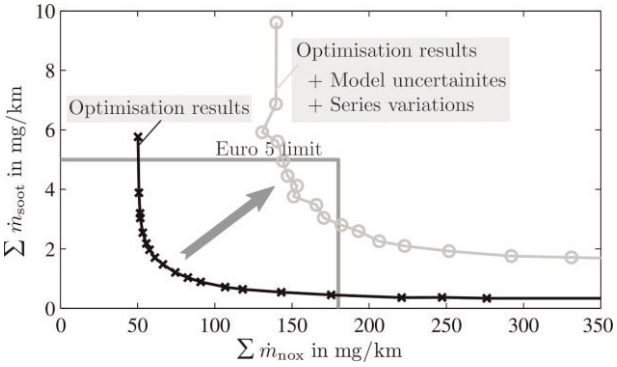

Fig. 9. Total emissions for the NEDC. Summed up emissions without model uncertainties and series variations (black) and with the worst case assumptions of model uncertainties and series variations (grey). Setpoints for simulation are taken from a separate local optimization in all engine operation points.

The black line shows the predicted emissions for setpoints derived from a local optimization of the engine. The grey line shows the emissions for the same setpoints with worst case assumptions for model uncertainties and series variations. It can be seen that the optimized prototype engine does fulfil the boundary conditions of the EU5 limits for various weights k_{NOx} and k_{soot} (black crosses inside the EU5 limit). However, if the worst case assumptions for model uncertainties and series variations are included, the EU5 limits are partially missed (grey circles). It is therefore important to consider these uncertainties in an early state of the optimization process. In the following model uncertainties and series variations are determined in the same way as introduced in Section 4.3 and are included in the boundary conditions of (26). Thus, the optimization criterion can be written as

$$\max_x J_{\text{global}} = \sum_{\text{j=1}}^{M} \frac{2\pi n_{\text{eng,j}}}{60} M_j(x) \quad \text{with}$$
$$\sum_{j=1}^{M} k_j k_{\text{NOx}} \left(\dot{m}_{\text{NOx},j}(x) + \sigma_{\text{NOx},j}(x) + \left| \frac{d\dot{m}_{\text{NOx},j}(x)}{dx} \right| \sigma_{\text{sensor}} \right) \le \text{NO}_{\text{x,limit}}$$
$$\sum_{j=1}^{M} k_j k_{\text{soot}} \left(\dot{m}_{\text{soot},j}(x) + \sigma_{\text{soot},j}(x) + \left| \frac{d\dot{m}_{\text{soot},j}(x)}{dx} \right| \sigma_{\text{sensor}} \right) \le \text{soot}_{\text{limit}} \tag{27}$$

This equation can then be optimized for a global optimization, taking the initial values from the optimized setpoints of a local optimization. Results for the global optimization without consideration of uncertainties as in (26) and for the global optimization with consideration of uncertainties as in (27) are shown in Fig. 10.

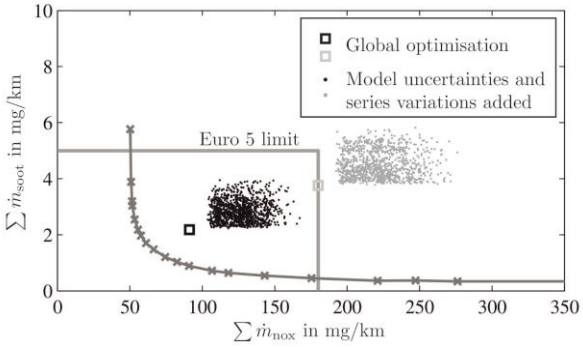

Fig. 10: Total emissions of the NEDC for setpoints derived from the global optimization with model uncertainties and series variations (black) and without (grey). The 1000 Monte-Carlo simulations are shown for the uncertainties for both cases under the assumption, that the occurrence of uncertainties is normally distributed.

The squares show the derived results. It can be seen that both squares are in the EU5 limits, whereat the optimized value of (26) (grey) is on the boundary conditions and the optimized value of (27) (black) has a safety distance to the boundaries. The occurrence of uncertainties is assumed to be normally distributed. Therefore 1000 realisations of uncertainties are added to the optimized values for both cases. It can be seen that if the uncertainties are not included in the optimization criterion (grey dots), the EU5 limits are missed for all of the realisations. However, if the uncertainties are considered all of the realisations are in the range of the limits (black dots). The optimization results for the two cases are J_{global}=1.87kWh if no uncertainties are regarded and J_{global}=1.80kWh if the uncertainties are regarded. Hence the compliance of limits for a series production is bought with a slight increase in fuel consumption. The results of this optimization are then optimal setpoints

$$\mathbf{x}_{\text{des}} = \left[m_{\text{air,des}}, p_{\text{2i,des}}, T_{\text{2i,des}}, \varphi_{\text{Q50,des}} \right] \tag{28}$$

for the control system of the gas path and fuel injection system, which determines the manipulated variables s_{egr}, s_t and φ_{MI} according to Fig. 4, partially using inverted models, see Sequenz (2013).

4.5 Smoothing of the Grid Maps

It might be necessary to smooth the resulting setpoints in practice to reduce actuating energy, wear of materials and guarantee a smooth engine running. Results with and without smoothing of the setpoints for the global optimization results are shown in Fig. 10 for the air mass per cycle m_{air} and the crank angle of 50% mass fraction burnt φ_{Q50}. Here the smoothing of the grid maps is performed after the global optimization by the training of a LOLIMOT model with four local models in the engine operation range. Thus the derived grid maps are smooth but are no longer optimal with respect to (27).

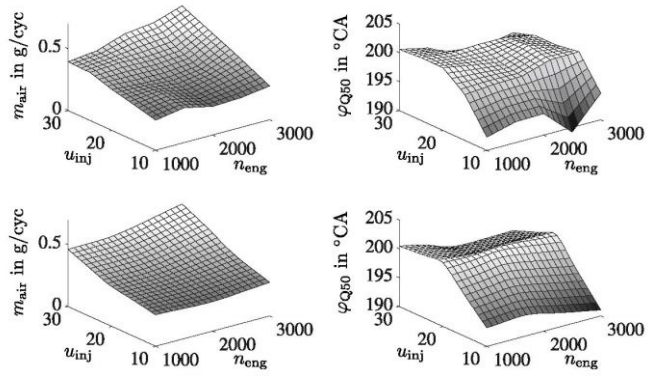

Fig. 11: Optimized setpoints for m_{air} (left) and φ_{Q50} (right) from the global optimization (top) and after a smoothing (bottom).

The smoothing can, however, also be performed during the optimization process by an implicit or an explicit regularisation. Thus, it can be reached that the results are still optimal setpoints with respect to the optimization criterion.

5. CONCLUSIONS

The increasing variability of modern internal combustion engines requires a systematic model-based development of control functions and their calibration. The first part has shown control-oriented structures and development steps from dynamic test bench measurements to optimized control design. The derived models from the bench measurements were utilised to optimise the emissions for a local optimization criterion. The results were then taken as initial values for a global optimization. Model uncertainties and series variations have a significant effect on the transferability of the global optimization results. Therefore, an optimization criterion which considers these uncertainties was introduced. The application example considered the quasi-stationary behavior for the control optimization of the NEDC cycle. The optimization of the dynamic behavior for the higher dynamic WLTC cycle is treated in Zydek (2016). After the global optimization a smoothing of the grid map was applied to guarantee a smooth engine running for load changes.

REFERENCES

Alberer, D., Hjalmarsson, H. and del Re, L. (eds.) (2012). *Identification for automotive systems*. Springer, London.

Eriksson, N. and Nielsen, L. (2014). *Modelling and control of engines and drivelines*. J. Wiley, Chichester, UK.

European Commission (2007). Regulation (EC) No 715/2007 of the European Parliament and of the Council, *Official Journal of the European Union L171*, 2007, 50, 1-15.

Guzzella, L. and Onder, C.H. (2010). *Introduction to modeling and control of internal combustion engine systems*. Springer, Berlin, 2nd edition.

Hafner, M. (2002). *Modellbasierte stationäre und dynamische Optimierung von Verbrennungsmotoren am Motoren-prüfstand unter Verwendung neuronaler Netze*. Fortschr.-Ber. VDI Reihe 12, 482. VDI Verlag, Düsseldorf.

Isermann, R. (2014). *Engine modeling and control*. Springer, Berlin.

Isermann, R. (ed.) (2010). *Elektronisches Management motorischer Fahrzeugantriebe*. Vieweg+Teubner, Wiesbaden.

Isermann, R. and Münchhof, M. (2011). Identification of dynamic systems. Springer, Berlin.

Kiencke, U. and Nielsen, L. (2005) *Automotive control systems*. Springer, Berlin, 2nd edition.

Kötter, H. (2008). Innovative Motorvermessung. Schnelle Motorvermessung mit optimierten Testsignalen. FVV Heft 853. FVV, Frankfurt.

Kruse, T., Kurz, S., and Lang, T. (2010). Modern statistical modeling and evolutionary optimisation methods for the broad use in ECU calibrations. *IFAC Symposium on Advanced Automatic Control*, München, Germany.

Mrosek, M. (2016). Model-based control of a turbocharged diesel engines. Internal report. Institute of Automatic Control, Technische Universität Darmstadt.

Mrosek, M., Sequenz, H., and Isermann, R. (2010). Control-oriented NOx and soot models for diesel engines. *IFAC Symposium Advances in Automotive Control*, München, Germany.

Nelles, O. (2001). Nonlinear system identification. Springer, Heidelberg.

Röpke, K. (2005). *DoE-design of experiments – Methoden und Anwendungen in der Motorenentwicklung*. Verlag moderne industrie AG, Landsberg/Lech.

Sequenz, H. (2013). Emission modeling and model-based optimization of the engine control. Diss. TU Darmstadt. Fortschr.-Ber. VDI, Reihe 8, No. 1222. VDI-Verlag, Düsseldorf.

Sequenz, H., Keller, K., and Isermann, R. (2012). Zur Identifikation mehrdimensionaler Kennfelder für Verbrennungsmotoren. *Automatisierungstechnik*, 60(6): 344–351.

Sequenz, H., Mrosek, M. and Isermann, R. (2010). Stationary global-local emission models of a CR-Diesel engine with adaptive regressor selection for measurements of airpath and combustion. *IFAC Symposium Advances in Automotive Control*, München, Germany.

Zydek, S. (2016). Optimal model-based diesel engine control for dynamic driving conditions. Symposium for Combustion Control, RWTH Aachen, June 15/16.